UNIVERSITÀ DEGLI STUDI DI TRIESTE

Investigating the fresh and mechanical properties of wood sawdust-modified lightweight geopolymer concrete

This is the peer reviewed (post-print) version of the following article:

Original
Investigating the fresh and mechanical properties of wood sawdust-modified lightweight geopolymer concrete / Nikoo, M., Hafeez, G., Faridmer, I., Ghasan, H., Bedon, C.. - In: ADVANCES IN STRUCTURAL ENGINEERING. - ISSN 1369-4332. - ELETTRONICO. - 26:7(2023), pp. 1287-1306. [10.1177/13694332231161103]

Availability:
This version is available at: 11368/3043919 since: 2023-04-26T06:57:19Z

Publisher:

Published
DOI:10.1177/13694332231161103

Terms of use:

Some rights reserved. More details in the PostPrint rights section below.

License:
Digital Rights Management not defined

Publisher copyright

-.-

(Article begins on next page)

26 October 2026

arTs Università degli Studi di Trieste
Archivio della ricerca – postprint

Investigating the fresh and mechanical properties of wood sawdust-modified lightweight geopolymer concrete

Nikoo Mehdi[1], Hafeez Ghazanfarah[1], Faridmer Iman[2], Ghasan F Huseien[3] and Chiara Bedon[4]

Abstract

Geopolymer concrete has developed as a potential alternative to ordinary Portland cement-based concrete, wherein various industrial by-products have been converted as beneficial spin-offs. Apart from appropriate compressive strength in the construction sector worldwide, the durability, sound absorption, thermal conductivity, and weight of concrete are also major concerns. Lightweight geopolymer concretes have gained attention because of their superior strength, durability, lower environmental impact, and sustainable characteristics. In this view, the current study examined the feasibility of using sawdust as a natural fine and coarse aggregate substitution in fly ash (FA)-granulated blast furnace slag (GBFS) based geopolymer concrete. Four mixes with a different percentage of sawdust (25, 50, 75, and 100) substituting natural aggregate were designed to examine the effects of sawdust on fresh and hardened features of geopolymer concrete compared to those conventional FA-GBFS-based geopolymer concrete with natural aggregate. Sodium silicate (NS) and sodium hydroxide (NH) (with NS/NH ratio of 0.75) were utilized to dissolve the alumina silicate from FA and GBFS. Informational models were developed using an experimental dataset to estimate the compressive strength of geopolymer concrete mix designs. Besides, using the weight of the developed network, a global sensitivity (GS) analysis was developed to identify the sensitivity of compressive strength to the waste sawdust content. Test results confirmed that by substituting natural aggregate with 100% sawdust, there was around a 35% decrease in compressive strength. Nevertheless, the sound absorption coefficient was increased by an average of 38% in frequencies range between 1800 and 2500 HZ, and thermal conductivity decreased by around 4.5 times once the natural aggregate was substituted by 100% sawdust.

Keywords

geopolymer concrete, waste sawdust, compressive strength, lightweight concrete

Introduction

Sawdust defines as agricultural by-products resulting from the wood industry once timbers are mechanically cut into diverse shapes and sizes. Dumping sawdust is a major environmental concern and requires large land concerning the large amount of waste produced by timber manufacturing processes in factories. Roughly the sawdust production in the USA, Germany, the UK, and Australia is estimated to be 64, 8.8, 4.6, and 4.5 million tonnes per year, respectively, where around 40% of these quantities are not recycled; indicating inadequacy in recycling strategies (Trømborg et al., 2013). One possible approach to tackle this problem and guarantee sustainable disposal as an environmental remedy is utilizing them efficiently in concrete/cement-based composites.

Following ACI regulation, lightweight structural concrete with low-density aggregate has an air-dried density of not more than 1850 kg/m^3 and compressive strength (after 28-days of curing) of more than 17 MPa (Institute, 2011).

[1]Department of Building, Civil and Environmental Engineering, Concordia University, Montréal, Canada
[2]Institute of Architecture and Construction, South Ural State University, Chelyabinsk, Russia
[3]Department of the Built Environment, School of Design and Environment, National University of Singapore, Singapore, Singapore
[4]Department of Engineering and Architecture, University of Trieste, Trieste, Italy

Corresponding author:
Chiara Bedon, Department of Engineering and Architecture, University of Trieste, Via Alfonso Valerio, 6/1, 34127 Trieste, Italy.
Email: chiara.bedon@dia.units.it

High-performance lightweight concretes (LWCs) attracted many researchers (Kockal and Ozturan, 2010; Sajedi and Shafigh, 2012; Sikora et al., 2020, Dixit and Pang, 2022). Following are summaries of some of the advantages of LWCs:

1. since the industrial by-products can be utilized in LWCs, it becomes economically feasible;
2. the reduction of weight facilitates the transport, casting, and erection of precast products;
3. since the larger pores in aggregates are unlikely to become saturated, the LWCs have better freeze-thaw resistance;
4. LWCs have lower thermal expansion and better sound absorption than ordinary Portland cement (OPC) concrete.

In recent years, the use of industrial by-products, including sawdust, to produce LWCs has attracted many researchers. The thermal traits of sawdust-based concrete were investigated (Ahmed et al., 2018; Sosoi et al., 2022; Huseien et al., 2019). It was show that the inclusion of sawdust in the concrete matrix relatively reduces thermal conductivity by around 20% compared to OPC-based concrete. Such a substantial reduction in thermal conductivity was attributed to the increased porosity and lowering the density of the LWCs produced by waste sawdust. Oyedepo et al. (2014)substituted fine aggregates with sawdust at different contents from 0% up to 100% in conventional OPC-based concrete and confirmed that the compressive strength of concrete could be negatively impacted by substituting more than 25% sawdust. Batool et al. (2021) investigated the effects of substituting natural fine aggregate with untreated sawdust (in the ratio of 10%–60%) on microstructure, mechanical properties, and hydration days. They confirmed that by increasing the sawdust content, there was a wider opening, crack formation, and interface gaps in the cement matrix. Besides, they conclude that the workability was reduced by increasing the sawdust substituting levels. Khan et al. (2020) investigated the mechanical strength and durability parameters of sawdust-based concrete (substituting natural aggregate with 5%, 10%, and 15%) subjected to elevated temperatures. Results showed substantial retention in compressive strength of sawdust-based concretes at elevated temperatures with partial spalling sensitivity. Besides, visual observation using micro-forensic signals demonstrates that sawdust-based concrete displays reduced thermal cracking in the macro, micro, and nanophase, compared to conventional OPC-based concrete. In their review document, Chowdhury et al. (2015) presented an overview of the research and investigation done from 1991 to 2012, on the use of wood ash as a partial replacement for cement in concrete. They summarized physical, chemical, and microstructural aspects as well as the effect of sawdust on properties such as water absorption, compressive strength, workability, bulk density, freeze-thaw, and acid resistance.

In recent years, geopolymer concrete has been introduced as an alternative to conventional Portland cement-based concrete with a much lower CO_2 footprint and better mechanical properties and durability. Geopolymer concrete and mortar are inorganic polymers based on alumina-silicates (AS_s), and calcium (C_aO) activated with an alkaline activator solution of sodium hydroxide (NaOH) and sodium silicates (Na_2SiO_3) (Adesina, 2020; Kantarcı and Maraş, 2022, Chowdary and Rao, 2022). The geopolymer concrete is environmentally friendly as it requires industrial by-products over its manufacturing (Maras and Kose, 2021). Fly ash (FA) is a coal combustion by-product that is contained the particulates that are driven from coal-fired boilers composed of flue gases, and granulated blast-furnace slag (GBFS) is attained by quenching molten iron slag from a blast furnace in water or steam, to create a glassy, granular material that is then dried and ground into a fine powder. These industrial by-products comprise Si, Al, and/or Ca, acting as binding material in geopolymer concrete. The previous literature confirms that the FA-GBFS-based geopolymer has excellent mechanical and durability features (Alharbi and Abadel, 2022; Algaifi et al., 2021; Asaad et al., 2022; Maras, 2021).

In geopolymer preparation, the geopolymerisation process needs an alkaline activator such as sodium/potassium silicate and sodium/potassium hydroxide or a combination of both alkaline (Palomo et al., 1999; Galdean et al., 2000). The utilization of an alkaline solution has been reported (Ruiz-Santaquiteria et al., 2012; Palomo et al., 1999), suggesting that the type of activator is significant in the geopolymerisation process. The high rate of reaction occurred using a soluble silicate, which differed from the usage of alkaline hydroxides. Xu Hua (Xu and Van Deventer, 2000) revealed that the response between the supply material and the solution increased by adding sodium silicate to sodium hydroxide. Moreover, they discovered that the sodium hydroxide (NaOH) solution is better than potassium hydroxide (KOH) due to its greater extent of material dissolution.

Alkali-activated materials are generally classified into two groups. The first includes the high calcium system with GBFS as a typical precursor and C-A-S-H type gel as the main reaction product (Brough and Atkinson, 2002). The second type is the low calcium system with Class F FA, POFA, and metakaolin as representative raw materials and N-A-S-H type gels within a three-dimensional network as the major reaction product (Granizo et al., 2002). Extensive research has been performed on these two systems to determine the role of activator type and alkali concentration (Yusuf et al., 2014a), the effect of the dosage of raw

materials (Deir et al., 2014), the effect of admixtures (Rashad, 2014; Duan et al., 2015; Makhloufi et al., 2015), the curing effect (Yusuf et al., 2014c), microstructure, mechanical properties, thermal properties and durability (Duan et al., 2015). Despite the excellent performances of both systems, there remain shortcomings for practical applications such as fast setting, high shrinkage of alkali-activated slag (Puertas et al., 2004; Palacios and Puertas, 2007), elevated curing temperatures demand, and relatively long setting times of alkali-activated aluminosilicates. Such disadvantages are overcome using a promising solution made of the blended alkaline systems (Na_2O–CaO–Al_2O_3–SiO_2 systems) which are produced by mixing calcium enriched precursors and aluminosilicates (Gao et al., 2015a, 2015b, 2015c; Yusuf et al., 2014b; Papa et al., 2014; Islam et al., 2014; Bagheri and Nazari, 2014).

For the present study, an extensive literature review indicated that the possible application of sawdust for producing geopolymer LWCs as sustainable building materials had not been extensively explored. No systematic research studies, however, could be retrieved in the open literature on the effects of sawdust on the durability and mechanical properties of geopolymer concrete. This study investigated the effects of natural aggregate substitution with sawdust on the fresh and mechanical properties of FA-GBFS-based concrete. Several FA-GBFS-based mix designs containing different levels of sawdust (0%, 25%, 50%, 75%, and 100%) replaced natural aggregates were developed. All the synthesized mix designs were analysed by several measures to examine the fresh, mechanical, and durability features. To address the shortcomings of existing international standards, an informational model was developed in the second stage of presently reported study, to predict the compressive strength of geopolymer concrete containing sawdust. More precisely, the model was developed using the shuffle frog leaping algorithm (SFLA) combined with a feed-forward (FF) neural network. To examine the accuracy and potential of the proposed SFLA model, multiple linear regression (MLR) and grey wolf optimizer (GWO) models were also developed, where several statistical metrics, including the mean square error (MSE) and the coefficient of determination (R^2), were utilized for evaluation purposes.

Experimental program

Materials

GBFS with high purity was prepared from Ipoh, Malaysia, and used to manufacture geopolymer concrete without further treatment. Unlike other supplementary cementitious materials, GBFS possesses both cementitious and pozzolanic properties. Meanwhile, Low-level Ca comprising FA (alumina-silicate by-product with a grey color) was attained from a Malaysian power station (Tanjung bin, Johor, Malaysia). This type of FA contained Ca (5.2%), silicate (57.2%), and Al2O3 (28.8%) and fulfilled the ASTM C618 requisites for FA class F (ASTM, 2015). The particle average for the FA and GBFS slag was 10 and 12.8 μm, respectively, which was tested by a particle size analyzer.

The physical features of both binding materials (GBFS and FA) were examind using the Brunauer Emmett Teller test with a specific surface area (18.1 m^2/g for FA and 13.6 m^2/g for GBFS) calculations. Figure 1 shows the X-ray diffraction (XRD, Rigoku, Singapore, Singapore) pattern of FA and GBFS. Detected intense XRD peaks of FA at $2\theta = 16 - 30°$ were because of the presence of Al_2O_3 and polycrystalline silica. Nevertheless, the eminent peaks at other angles were because of the existence of mullite crystallites and quartz. On the other hand, the amorphous nature of GBFS is responsible for the non-appearance of any sharp peak. The existence of silica and Ca positively impacted the composition of GBFS and improve the mechanical properties of geopolymer concrete. At the same time, using FA in geopolymer concrete boosts the low level of Al_2O_3 (10.49%) in the GBFS slag.

To manufacture ordinary Portland cement concrete (control sample), river sand was utilized as the fine aggregate in all mix designs that were washed with fresh water to remove the silts and to remove the moisture, oven drying at 60° for 24 h based on ASTM C117 (ASTM, 2006) and ASTM C33–33M (Aggregates) protocols. The highest particle size, specific gravity, and fineness modulus of the prepared sand were recorded 2.36 mm, 2.6, and 2.9 mm respectively. Crushed garnet stone from a mine was used in all mix designs as a coarse aggregate where the maximum size was limited to 8 mm. The size of coarse aggregate significantly impacted the mechanical properties of conventional concrete.

The sawdust (No. 6013) was attained from the wood industry in Johor province in Malaya, as shown in Figure 2. This local agro-waste has a density of 174 kg/m^3 and a maximum size of 2.36 mm for the fine aggregate and 182 kg/m^3 and a maximum size of 6 mm for the coarse aggregate, enhancing the production of LWC. Sawdust was treated before its mixing. The process of sawdust treatment included soaking the sawdust for 1 hour in a container filled with water, and then for draining water from the sawdust, it was kept 15 min on the mesh. The natural aggregates were replaced by different levels of sawdust wastes (0%, 25%, 50%, 75%, and 100%) at the realistic working level with the appropriate physical condition to make the lightweight geopolymer concretes.

Table 1 presents the loss of ignition (LOI) and chemical composition of utilized sawdust in this study. As shown in Table 1, the main component of the sawdust is cellulose (87% of the total mass) and low quantities of Al_2O_3 and

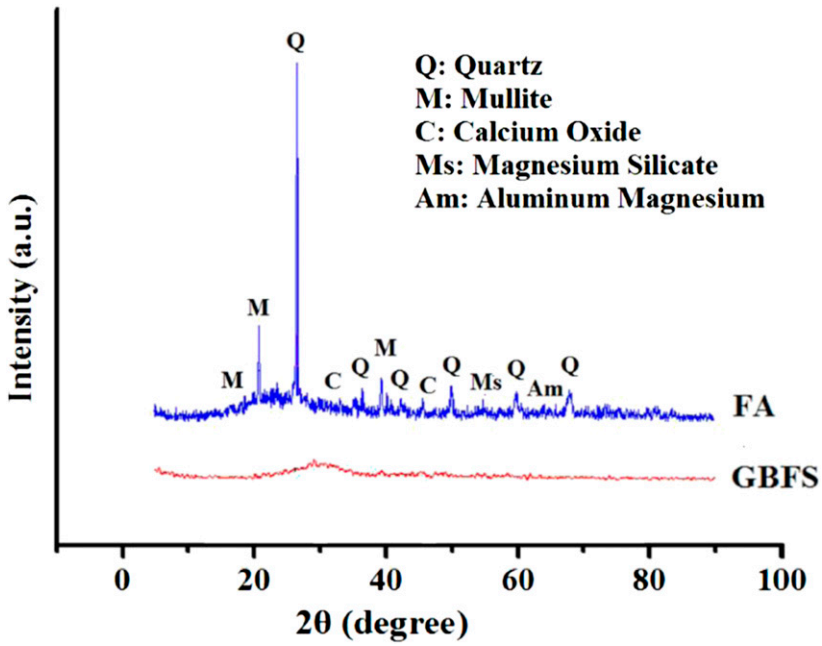

Figure 1. XRD diffractograms of GBFS and FA.

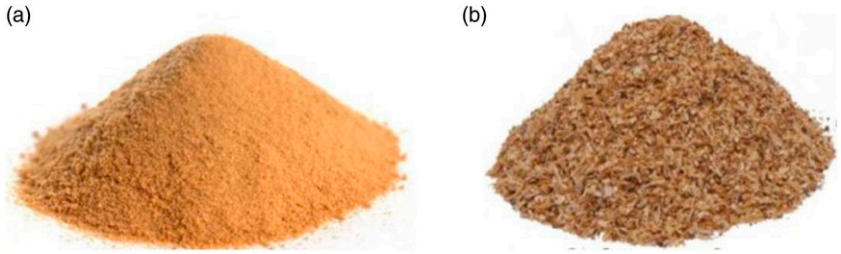

Figure 2. (a) Fine sawdust aggregate and (b) coarse sawdust aggregate.

Table 1. Compositions of the utilized sawdust (%).

Cellulose	Al_2O_3	Fe_2O_3	CaO	MgO	K_2O	LOI
87.0	2.5	2	3.50	0.23	0.01	4.76

CaO. The sawdust's LOI ratio was recorded at 4.76% (out of the total mass).

Sodium hydroxide (NH) and sodium silicate (NS) were utilized in this study to prepare the alkaline solution (S). This solution dissolves the alumina-silicate of FA and GBFS, and the following steps were followed to prepare it:

1. Analytical-ranking NH pellet (98% purity) was dissolved in water to obtain an alkaline solution with 86.3% of H_2O (2 M) and 13.7% of Na_2O;
2. By mixing H_2O (55.80 wt.%), SiO_2 (29.5 wt. %), and Na_2O (14.70 wt.%), NS mixture was produced;
3. In the first phase, the NH solution (2 M) was kept at ambient temperature for 24 h and then mixed with NS solution (obtained in the previous step) to prepare the alkaline solution with a modulus (Ms of SiO_2:Na_2O) of 1.21.

Mix designs

To study the effects of sawdust on the mechanical properties of geopolymer concrete, several mix designs with different compositions were prepared, as shown in Table 2. The NS/NH ratio was kept constant at 0.75 for all the alkali solutions. In conventional geopolymer concrete, different percentage of FA and GBFS (as sources of SiO_2, Al_2O_3, and CaO) was used; however, the ratio of FA to GBFS in sawdust-modified geopolymer concrete remained constant at 2.33. Four substitution contents (sawdust substituting natural aggregate by 0.25%, 0.5%, 0.75%, and 100%) were

Table 2. Studied geopolymer concrete mix designs.

	Binding	Activator	Aggregate (kg/m^3)			
Mix	FA/GBFS	NS/NH	Sand	Coarse	Fine sawdust	Coarse sawdust
S0-1	0	0.75	844	756	0	0
S0-2	0.428	0.75	844	756	0	0
S0-3	0.666	0.75	844	756	0	0
S0-4	1	0.75	844	756	0	0
S0-5	1.5	0.75	844	756	0	0
S0-6	2.33	0.75	844	756	0	0
S0-7	2.33	0.75	845	950	0	0
S25	2.33	0.75	634	712	22	26
S50	2.33	0.75	422	475	45	47
S75	2.33	0.75	211	237	67	71
S100	2.33	0.75	0	0	90	95

considered to study the effects of sawdust on the fresh and mechanical properties of modified geopolymer concrete.

Tests procedure on fresh and hardened geopolymer concrete

Fresh properties. The first phase of preparing the mix designs involved blending binary binder (GBFS and FA) and then gradually mixing with aggregates until the homogenous mixture was prepared. In the second phase, the alkaline activator solution, consisting NaOH + Na_2SiO_3 with ratios of 0.75, was prepared, and once it became cool at ambient temperature for 24 h, it was mixed with an already prepared homogenous mixture. Subsequently, the fresh mixture was prepared, and relevant tests on fresh properties, slump test and setting time, were conducted. To examine the mechanical properties, the fresh concrete was first cast in moulds in three layers, and using vibration table each layer was consolidated for 30 s to guarantee that air bubbles evacuated. After casting, the specimens were cured at ambient temperature (27 ± 1.5) and relative humidity of 75% for 24 h. Then, the specimens were demoulded and kept till testing time.

Fresh properties were examined in line with the conditions of ASTM C143 and C191 protocols (Standard, 2013, Standard, 2004) for the slump and setting time. Setting times of geopolymer concretes are categorized into initial and final ones. The duration between the mixing of binder and partial loss of plasticity introduces the initial setting time, whereas the required time to achieve an acceptable hardened form to sustain a given pressure introduces the final setting time. Vicat is a frequently used method to estimate the setting times in compliance with ASTM C191 requirements. The Vicat method allows a 1-mm Vicat needle to settle into the geopolymer past. The Vicat initial time of setting is considered as the time elapsed between the initial mixing of binding materials and alkaline solution and the time when the penetration is at 25 mm. The Vicat final setting time is measured as when the needle does not sink visibly into the fresh concrete.

Compressive strength. The compressive strength was measured using cubic-shaped molds (100 × 100 × 100 mm) that were cured for 90 days in compliance with ASTM C579 Standard (2012) guideline. The compressive strength test was conducted following the ASTM, 2020 C109-109M guideline (ASTM), where three specimens were tested at each curing age (7, 28, and 90-days). The compression load at a constant rate (2.5 kN/second) was applied to the specimens till their failure. The machine automatically recorded specimens' compressive strength and density based on the imputed specimen dimensions and weight.

Sound absorption. Acoustic absorption coefficients typically describe the potential of absorbing sound energy. In this study, the impedance tube technique was utilized to identify the sound absorption and impedance of the sawdust-modified geopolymer concrete. This technique uses a two-microphone transfer-function to record the absorption coefficient in the frequency range of 100–6000 Hz, as shown in Figure 3.

Heat transfer measurement. The buildings and construction sectors combined are responsible for almost one-third of total global final energy consumption and nearly 15% of direct CO_2 emissions. In buildings construction sectors, energy can be saved through installing thermal insulation, which saves energy and provides substantial financial benefits. The previous research acknowledged that thermal insulation and proper building orientations

Figure 3. Impedance tube instrument.

could save up to 20% energy (Al-Homoud, 2005; Natephra et al., 2018).

The actual heat resistance of insulating building materials is inversely proportionate to humidity and temperature. Choosing an appropriate technique for recording the concrete thermal conductivity is essential to accurately estimate buildings' energy consumption. In this study, the heat transfer was recorded for the standard cylindrical sample with150 millimeter diameter and 300 mm height. At the age of 28-days of curing, the outer surface of the sample was covered using a plastic sheet, to avoid the air humidity entry. To protect the thermocouple from unforeseen impacts, a PVC pipe with a 20 mm diameter was also employed. All the specimens were mounted in a water container with a temperature of 34°C where it steadily increased to 100°C, and the first recording was performed. Then the heater was switched on to measure the central temperature of the samples using the K thermocouple (connected to data loggers and computer). The heater's temperature was increased during the immersion of samples in water, thereby increasing the water volume. The increasing of temperature was recorded at close intervals in the first 24 h up to 100°C. Nevertheless, the heat was recorded regularly till the water temperature reached boiling. Figure 4 illustrates the heat transfer measurement technique used in this study.

Results and discussion

Slump and setting time

Figure 5 illustrates the slump values of all studied mix designs. The results confirm that by increasing the sawdust content substituting natural aggregate, there is a decrease in slump value. The average slump value for conventional geopolymer concrete with natural aggregate was recorded at 140 mm, whereas by substituting all natural aggregate with sawdust, the slump decreased by around 55% and reached 75 mm. According to EFNARC standard (EFNARC, 2002), the mixtures with 40%–60% FA can be classified as slump flow class II, suitable for common building components, i.e., columns, beams, slabs, etc. Once FA content increases beyond 60%, the flow ability of the mix designs decreases. This fact is shown in Figure 5, where the slump value tends to decrease in mix design S0-5 with the FA/GBFS content of 1.5. Typically, the concrete workability was reduced with the rise in the sawdust amounts in the mixtures. Nevertheless, the influence was more prominent at higher sawdust content (100%). Generally, the workability of the concrete was affected by the specific surface area of the sawdust and the high water demand with a high level of sawdust in the matrix (Alabduljabbar et al., 2020; Al-Fasih et al., 2021).

Figure 6 illustrates the initial and final setting times of all studied mix designs. The results confirmed that both the initial and final setting times were decreased by increasing the sawdust content. The initial and final setting times of conventional geopolymer concrete with FA/GBFS ratio of 2.33 (mix design S0-7) were recorded 38 and 60 min, whereas by substituting all natural aggregate with sawdust, these values decreased and were recorded 25 and 43 min; around 40% decrease. This issue can explain by the fact that the sawdust aggregate influences the geopolymerization development, and the dissolving of calcium and alumina-silicate leads to demanding more water. Besides, the inclusion of sawdust in geopolymer concrete reduced pH due to the decomposition of lignin intervened by the pH changes in the alkaline solution. These results comply with the findings of Duan et al. (2016), where setting time was decreased for the concrete prepared by sawdust aggregate. The results also confirm that low-content FA mix designs have lower setting times, where in mix design S0-1 with 100% GBFS as binding material, the final setting time was recorded at only 10 min. The high absorption of sawdust into an alkaline solution imparted high viscosity to the mix, which was hardened rapidly. Whilst, the inclusion of sawdust in concrete mixtures with comparatively higher water absorption than river sand and gravel hardened the alkaline solution activated mixes more rapidly and decreased the setting time because of the adsorption of additional water by sawdust.

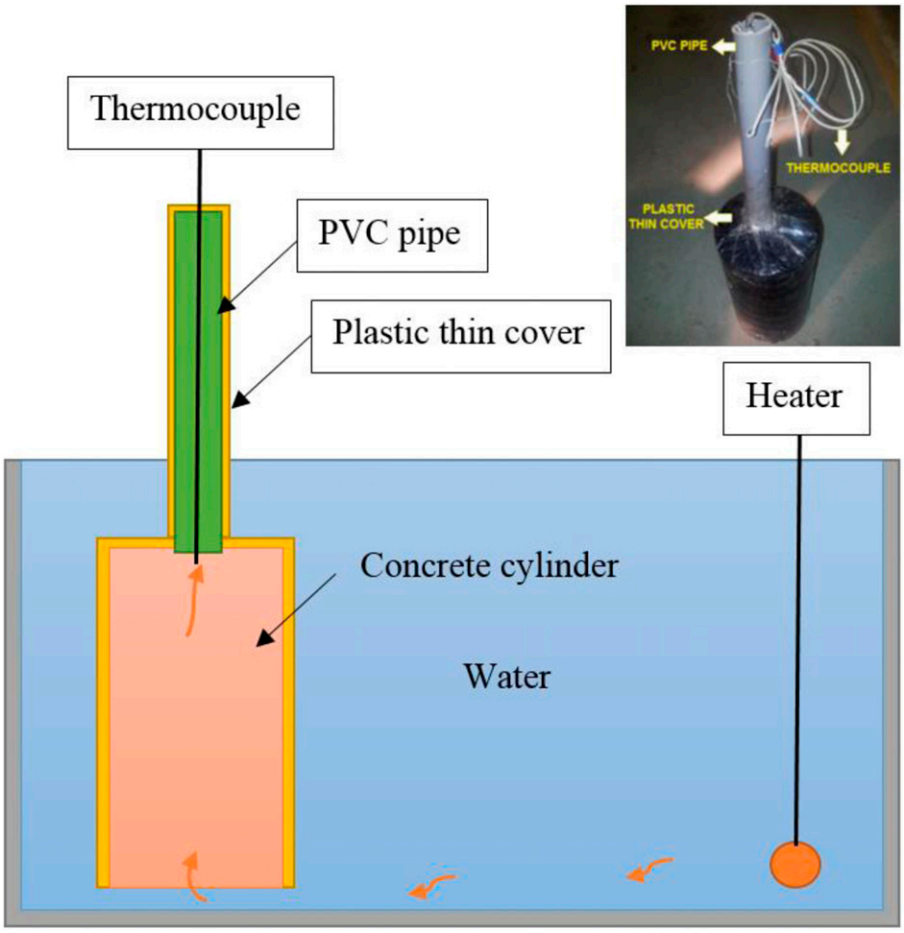

Figure 4. Heat transfer measurement.

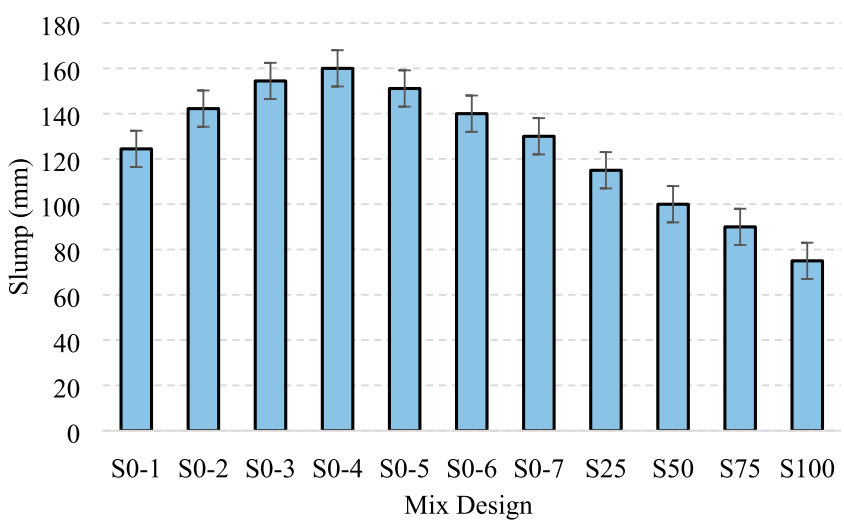

Figure 5. Slump value of all studied specimens.

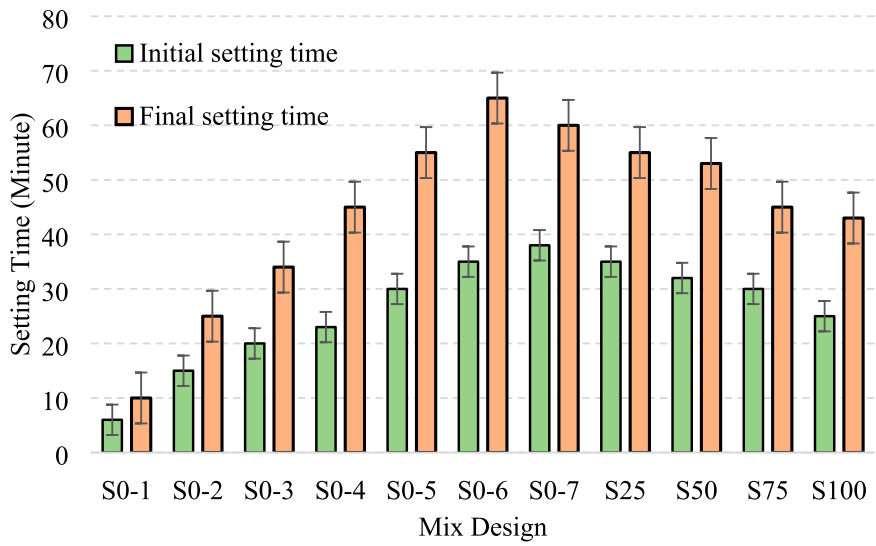

Figure 6. Initial and final setting time of all studied specimens.

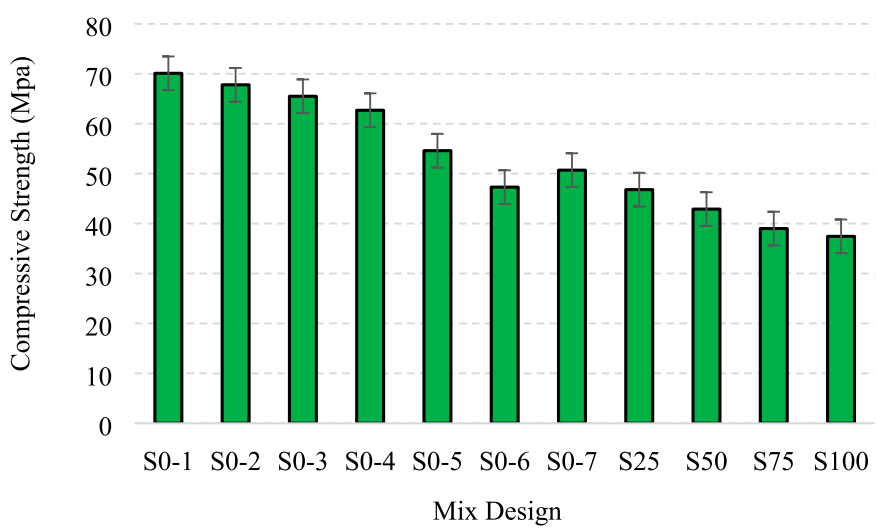

Figure 7. Compressive strength of all studied specimens (at the age of 28-days).

Compressive strength

Figure 7 illustrates the 28-days compressive strength of all mix designs considered in this study. The results confirmed that there is a contradictory relationship between compressive strength and sawdust content. In conventional geopolymer concrete with FA/GBFS ratio of 2.33 (mix design S0-7), the compressive strength was recorded 50 MPa, whereas by substituting all natural aggregate with sawdust, this value declined by 35% and was recorded 37 MPa. In conventional FA-GBFS-based concrete, increasing the GBFS percentage led to an increase in compressive strength. This behaviour may be attributed to incorporating GBFS forms many C-S-H gels while generating considerable heat, accelerating the geopolymerization process (Karamanova et al., 2011). Besides, the GBFS contains many calcium ions with enormous electrostatic attraction and charge neutralization capability compared with sodium ions, accelerating the formation of amorphous aluminosilicate gels and decreasing the setting time of geopolymers (Li et al., 2021).

This reduction in compressive strength using sawdust aggregate can explain by the fact that there is a weaker bond between aggregate and paste because of the existence of organic matter. Besides, the lack of pozzolanic particles in the sawdust negatively impacted the strength

development. Nevertheless, sawdust small particles and wood fibers may have filled many gaps between and within them each other, thus enhancing stress transfer between both materials. This finding is in line with the previous literature of Martínez-García et al. (2019), and González-Fonteboa et al. (Rojo-López et al., 2022). The results also confirmed that the inclusion of FA in the mix design reduced compressive strength by around 26%, varying with the content of FA. The low ratio of CaO to SiO_2 and Al_2O_3, the filling effect of FA particles, and the deceleration of the binder hydration led to the reduced compressive strength of mixtures containing FA.

Sound absorption

The acoustic absorption coefficients describe the potential of materials to absorb sound energy. Figure 8 displays the sawdust effect content on the sound absorption coefficient of studied sawdust-modified geopolymer concrete. The frequency range between 0 and 5000 Hz for testing all specimens. The results confirm that sawdust-modified geopolymer concrete possessed a higher potential to absorb sound energy in the range varies 500–3000 Hz. Substituting 100% natural aggregate with sawdust increased the sound absorption coefficients from 0.43 to 0.74. This issue can explain by the fact that sawdust provides more interconnecting voids at diverse length scales inside the geopolymer concrete matrix (Memon et al., 2017; Mishra and Jena, 2021). In the high-frequency domain, these permeable materials presented an enhanced sound absorption, especially concerning decreasing the concrete density that led the frequency to change to higher values. These findings comply with previous literature (Aliabdo et al., 2015; Park et al., 2005), as they acknowledge that materials' density and porosity highly impact the sound absorption capacity. They confirmed that the low density and high porosity would influence the energy absorption by the friction produced in the walls of permeable structures; presenting a higher value of sound absorption coefficient.

Thermal conductivity

To examine the thermal features of the sawdust-modified geopolymer concrete, the heat transfer time was measured at the 28-days of curing age, as shown in Figure 9. The results confirm that the thermal conductivity decline with the increase in sawdust content. By substituting all natural aggregate with sawdust, 188 min was required for heat transfer compared to 36 min for specimen made with 100% natural aggregate. Similar to sound absorption, an appropriate thermal conductivity of sawdust-modified geopolymer concrete directly correlates with its density and growth in the total porosity and thus reduces the thermal conductivity. The previous research also acknowledged

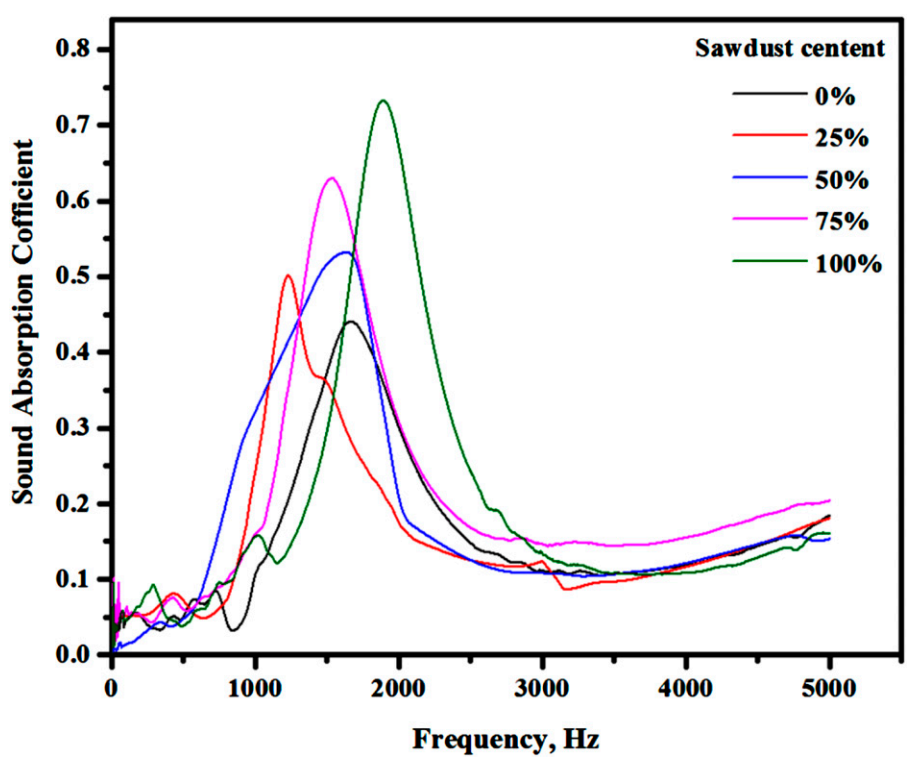

Figure 8. Sound absorption coefficients of the sawdust-modified geopolymer concrete.

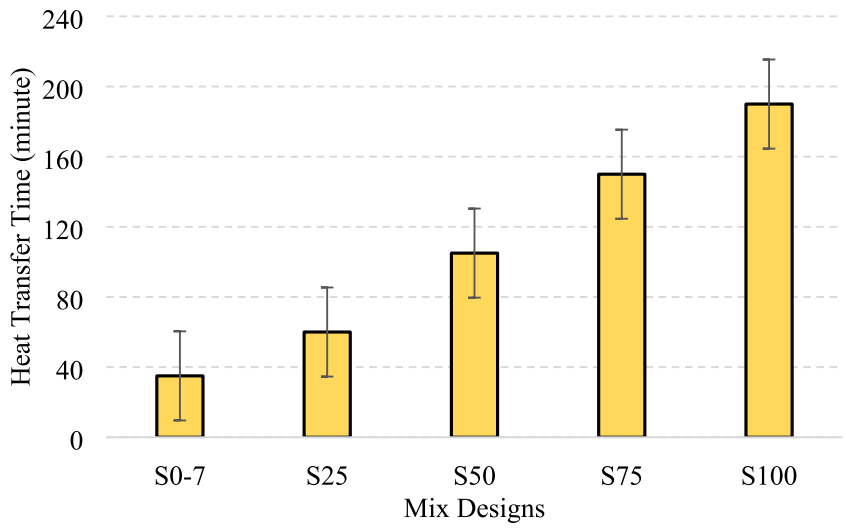

Figure 9. thermal conductivity of sawdust modified geopolymer concrete.

that a reduction in the thermal conductivity might be attributed to the convection development where geometry within the concrete matrix, the pore density, and spreading play an important role. Besides, according to available literature (Clarke, 2003), low thermal conductivity may also be attributed to the phenomenon known as convection, which is associated to the quantity and geometry of pores generated inside the concrete matrix (Clarke, 2003).

Developing informational model to estimate compressive strength

ANN learns from experience and generalizes the achieved knowledge of new data that are still unfamiliar to the model (Adeli, 2001; Flood and Kartam, 1994). ANN has been originally designed based on the biological brain structure; it consists of several neurons operating locally to find the best solution to a definite problem. ANN achieves new knowledge by learning using a simplified human brain-like approach in customary computations; this algorithm captures the underlying mechanisms within a dataset. The multilayer feed-forward network employed in the present paper is, in fact, a consistent and widely-utilized ANN structure. This network involves three different layers: (1) the input layer in which the data are introduced to the network, (2) the hidden layer(s) in which the network processes the data, and (3) the output layer in which the network results are created. In this system, each of the layers contains a group of nodes (neurons) coupled to the proceeding layer. Within the output and hidden layers, the nodes consist of three elements, i.e., activation function, weights, and biases that could be either continuous, linear, or nonlinear. A standard activation function involves the linear functions (Poslin, Purelin) as well as nonlinear sigmoid functions (Logsig, Tansig) (Nikoo et al., 2018). After determining the architecture of a feed-forward ANN (i.e., the number of layers, number of neurons within each layer, and activation function for each layer), training algorithms need to optimize the weight and bias levels. The backpropagation (BP) algorithm is one of the most dependable ANN training algorithms; capable of distributing the network error to achieve the best fit or minimum error (Haykin, 2007; Bishop, 2006).

This research develops an ANN combined with a Shuffled Frog Leaping Algorithm (SFLA) to predict the compressive strength of sawdust-modified geopolymer concrete. Using this informational model, it is also possible to determine the sensitivity of the compressive strength to the sawdust content.

SFLA features

The SFLA is developed on the memetic evolution of frog colonies searching for food. SFLA combines the genetic evolution-based memetic algorithm and the qualities of the social intelligence-based particle swarm optimization (PSO) algorithm. In this algorithm, frogs population represents a set of possible results; once the frog group is packed up into some memeplexes, each represents a various culture. Generally, frogs are motivated to enclose the best frog, a local optimum; some of the affiliates of a memeplex are categorized as a sub-memeplex to evade their merging to the local optimum. The frog that possessed the weakest position should evolve. After a specific number of memetic iterations, the memeplexes are shuffled as a population. The local search and shuffling procedure continue until the solution satisfies the needed index or the evolution generations are completed. Details of the SFLA steps can be schematized as follows (Liang et al., 2016):

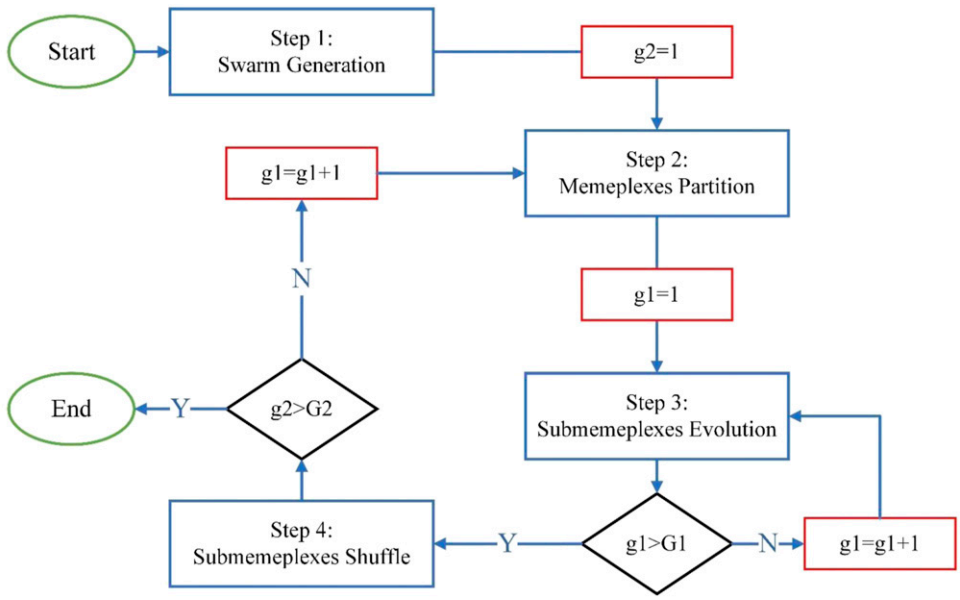

Figure 10. Flowchart of shuffled frog-leaping algorithm.

Step 1: swarm generation; Step 2: memeplexes partition; Step 3: submemeplexes generation; Step 4: submemeplexs evolution; Step 5: memeplexes shuffle. The implementation flow of the SFLA is shown in Figure 10 (Liang et al., 2016).

Characteristic and correlation of input/output variables

The dataset and its features are essential for developing the informational model. The independent input variables in the used dataset include curing age, FA/GBFS ratio, NS/NH ratio, and aggregate (sand, coarse, sawdust fine, and sawdust coarse) content, which produce a 6×1 matrix, while the dependent output parameter includes the compressive strength which develops a 1×1 matrix. The properties of input/output variables are given in Table 3.

Figure 11 displays this study's correlation matrix developed for input/output variables. To evade any deviation in the results, the input/output parameters were first normalized using equation (1).

$$X_n = \frac{2(X - X_{\min})}{X_{max} - X_{mix}} - 1 \tag{1}$$

where X_n is the normalized variable value, $X_{\max}$ and $X_{\min}$ is its maximum and minimum value, *and* X is the variable's real value.

Figure 12 shows a probability Plot of the output parameter in which this plot illustrates the range of compressive strength.

Network structures and statistical indices

Since a total of six input variables exist, the proposed SFL-ANN model takes six neurons in the input layer. 70% of the dataset was used for network training, and the remaining 30% was considered for network performance control. This data partition provided the best training outcome and robust model testing and validation. The features of the SFLA algorithm parameters are illustrated in Table 4.

The present study determined the number of neurons in the hidden layers according to equation (2).

$$N_H \leq \min\left(2N_I + 1; \frac{N_{TR}}{N_I + 1}\right) \tag{2}$$

where N_{H} is the number of neurons in the hidden layer(s), N_{I} is the number of input parameters, and N_{TR} is the number of training samples in the database.

The Levenberg–Marquardt training algorithm and hyperbolic tangent transfer function were used in all networks. Moreover, several statistical metrics, including the average absolute error (*AAE*), coefficient of determination (R^2), and variance account factor (*VAF*), which are expressed in equations (3 to 5), were used to evaluate the performance of the different network topologies.

$$AAE = \frac{\left|\sum_{i=1}^{n} \frac{(O_i - P_i)}{O_i}\right|}{n} \tag{3}$$

Table 3. Characteristic statistics of geometrical and mechanical parameters of the studied database.

Statistical index	Unit	Type	Max	Min	Average	STD
Age	Days	Input	90.0	7.0	41.7	35.8
FA/GBFS	Ratio	Input	2.3	0.0	1.6	0.9
Sand	kg/m^3	Input	845.0	0.0	652.4	295.5
Coarse	kg/m^3	Input	950.0	0.0	628.2	270.4
Fine sawdust	kg/m^3	Input	90.0	0.0	20.4	31.4
Coarse sawdust	kg/m^3	Input	95.0	0.0	21.7	33.2
Compressive strength	MPa	Output	78.0	32.0	54.9	11.9

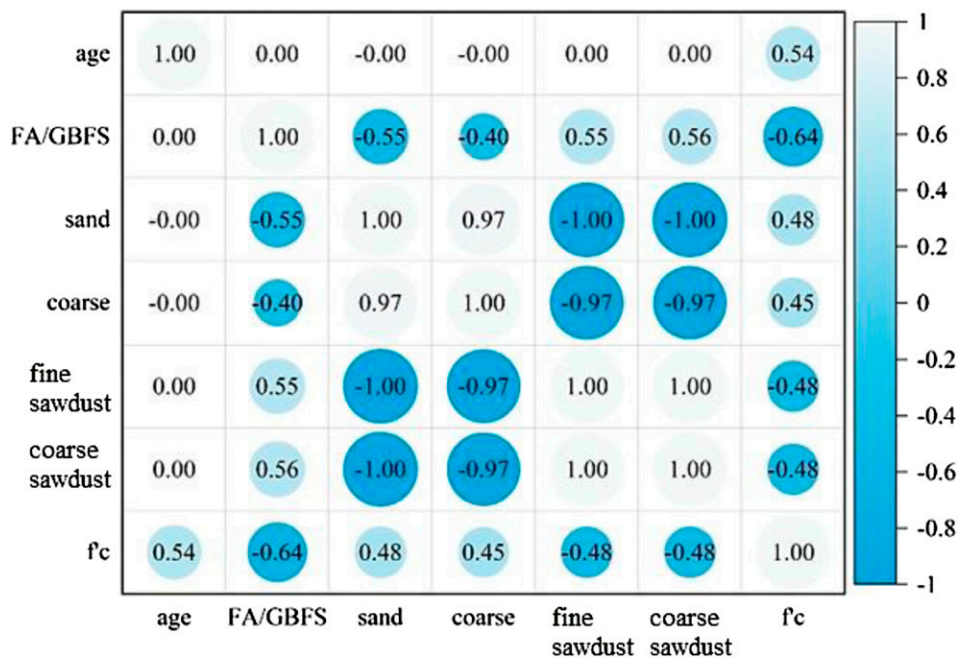

Figure 11. Correlation matrix for input/output variables.

$$R^2 = \frac{\sum_{i=1}^{n} \left(y_{i(model)} - \bar{y}_{(Actual)}\right)}{\sum_{i=1}^{n} \left(y_{(Actual)} - \bar{y}_{(Actual)}\right)} \quad (4)$$

$$VAF = \left[1 - \frac{var(O_i - P_i)}{var(O_i)}\right] \quad (5)$$

Overall, 20 different ANN architectures with two hidden layers have been developed and trained using the shuffled frog-leaping algorithm. It was found that the network with a 6-4-6-1 topology achieved the lowest error values for *AAE* and the highest value of *VAF* and R^2 in both the training and testing phase to estimate the output parameter, as shown in Figure 13.

Figure 14 illustrates the proposed 6-4-6-1 topology of the feed-forward neural network with two hidden layers, six input variables, and one output parameter.

Multiple linear regression and gray wolf optimizer models

To examine the reliability of the proposed hybrid SFL-ANN model, a gray wolf optimizer model combined with an ANN (GWO-ANN) and a MLR model were also used in this study.

In the MLR model, some independent parameters mainly influence the dependent variable, as per equation (6), where y is a dependent or output parameter and x_1, x_2,

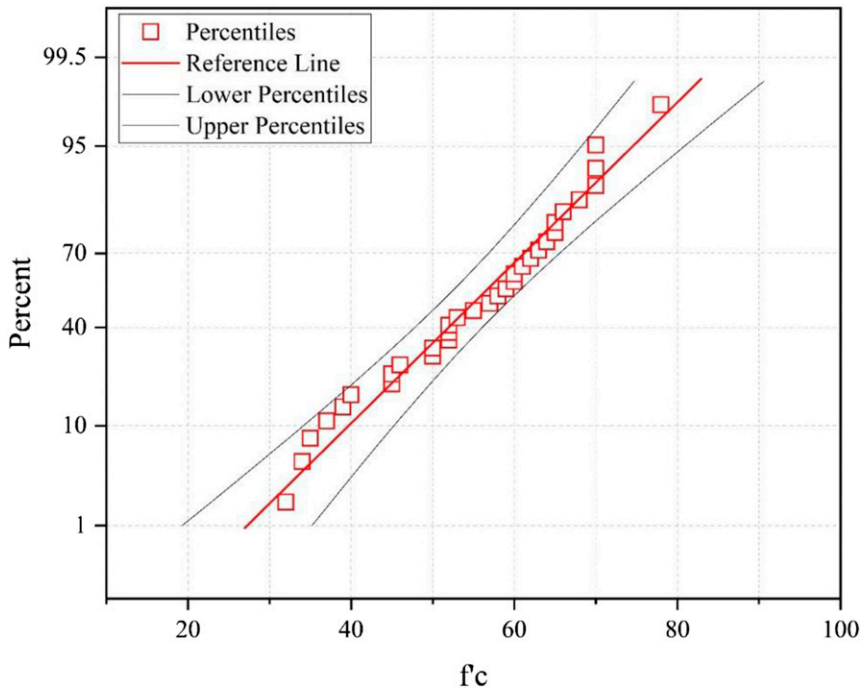

Figure 12. probability plot for input variable compressive strength.

Table 4. Shuffled frog-leaping algorithm.

Parameter	Value	Parameter	Value
Memeplex size	7	Number of parents	2
Number of memeplexes	3	Number of Offspring's	3
Population size	Memeplex size * number of memeplexes	Maximum number of iterations	5

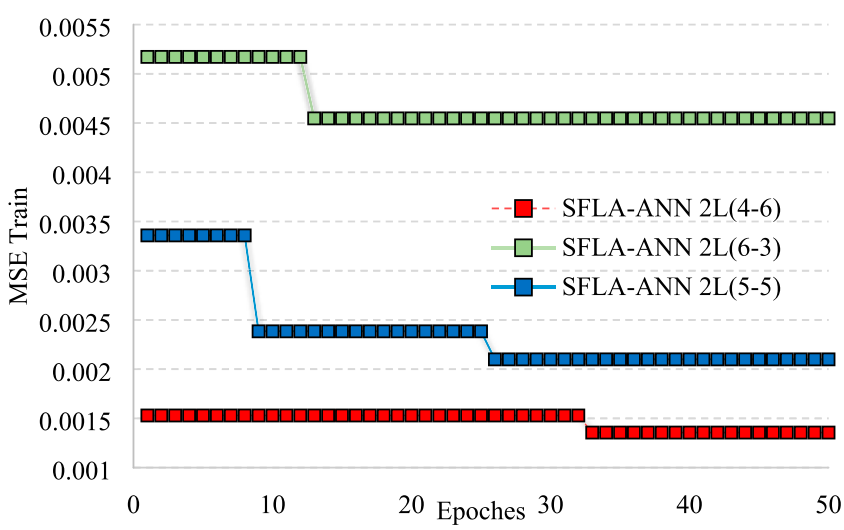

Figure 13. Performance of the best three ANN architectures trained with the SFL algorithm.

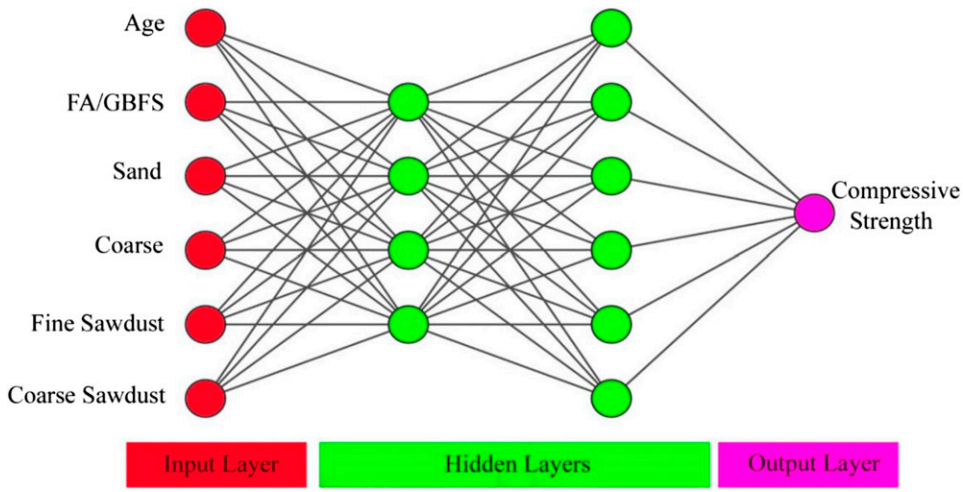

Figure 14. Proposed 6-4-6-1 topology to determine the compressive strength of modified-sawdust geopolymer concrete.

…, are independent input parameters. a_1, a_2, … are coefficients of the equation.

$$y = f(x_1, x_2, \ldots) \rightarrow y = a_0 + a_1x_1 + a_2x_2 + \ldots \quad (6)$$

Equation (7) shows the most appropriate coefficients for the MLR model for estimating the compressive strength.

$$Compressive\,strength = -184 + 0.179\,age - \frac{11.9FA}{GBFS} + 0.227sand + 0.0743coarse + 1.83fine\,sawdust + 0.87coarse\,sawdust \quad (7)$$

The GWO-ANN was also developed to optimize the different topologies in which the most accurate result was selected according to statistical metrics defined in equations (3 to 5). The features of the GWO parameters used to train different neural network topologies are given in Table 5.

Table 5. Grey Wolf Optimized (GWO) parameters.

Parameter	Value
Max generations	300
Search agents	10

Another visual representation of the comparison between the performance of the novel proposed SFL-ANN model against MLR and GWO-ANN models is the Taylor diagram, shown in Figure 16. This diagram represents a graphical diagram of the adequacy of each studied model using RMS, the SD, and the correlation coefficient. The results confirmed that the closest prediction of the compressive strength to the point representing the actual experimental data was attained by the SFL-ANN model developed in the present study. The MLR model estimated higher RMS and SD values, indicating a relatively low accuracy in estimating the experimental data compared to the GWO-ANN model.

Accuracy of proposed SFL-ANN model

Figure 15 compares the experimental results and the equivalent predictions of the SFL-ANN computational intelligence model and calculations of the MLR and GWO-ANN models considered herein. It is clear that the SFL-ANN model achieved more reliable estimations of the compressive strength compared to that of the MLR and GWO-ANN models.

The statistical metrics also acknowledged the capability of SFLA-ANN model to estimate the compressive strength of sawdust-modified geopolymer concrete against MLR and GWO-ANN models, as shown in Table 6.

Sensitivity analysis of compressive strength to sawdust content

This section examines the sensitivity of the drift capacity relevant to the LS3, δ_{LS3}, to the wall geometrical and reinforcement properties (L_w, h_{eff}, h_{eff}/L_w, ρ_v, ρ_h, σ_n). Sensitivity analysis (SA) captures how significantly changing input variables influence the output. In general, two types of SA exist, i.e., local and global. The former emphasizes upon the local influence of specific input variables on global appearance. The global sensitivity analysis (GSA) examines the effect of a particular input variable over the whole 3-D range and reveals the indecision of the output produced by input

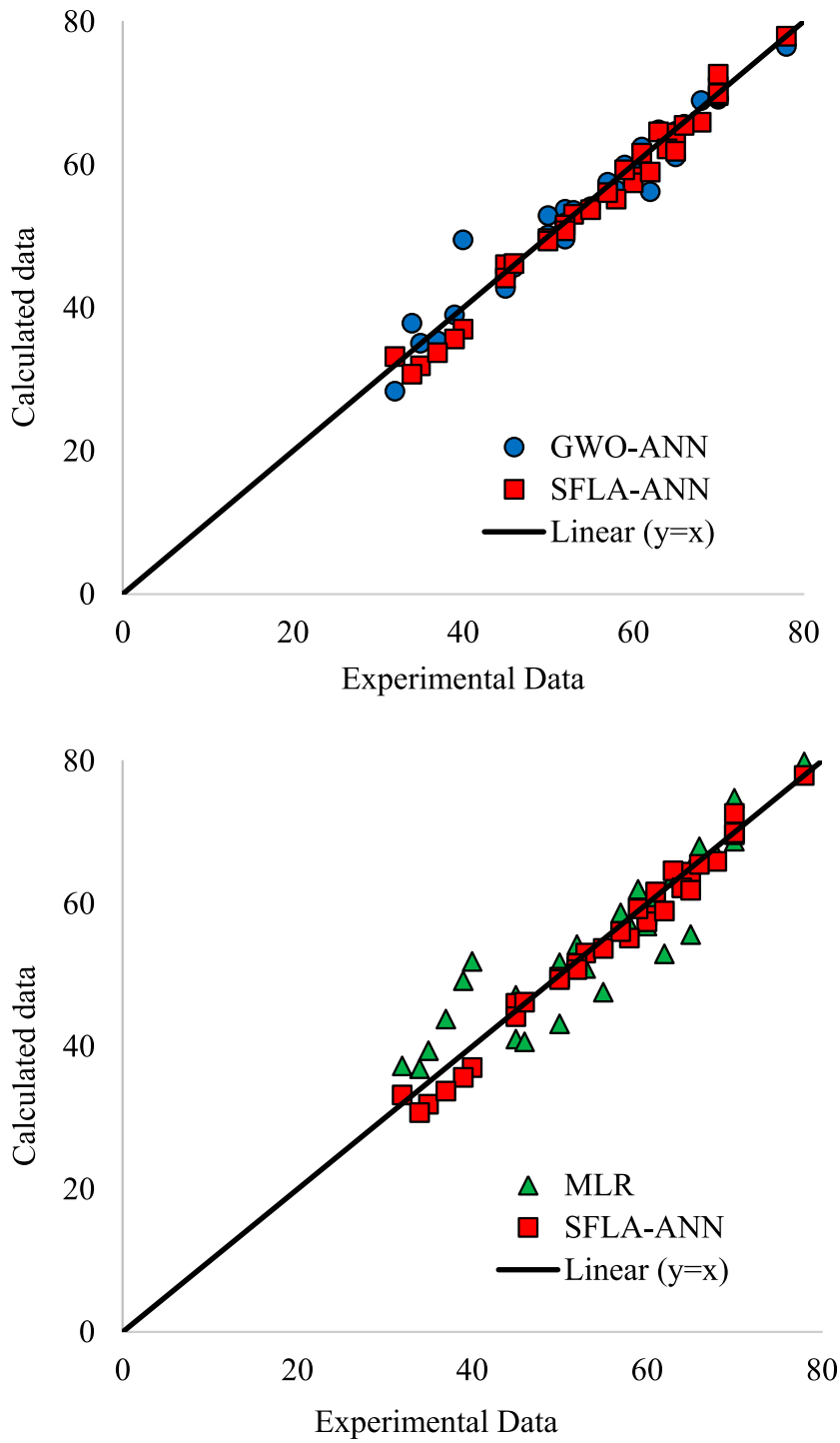

Figure 15. Comparison between experimental results and model predictions of the compressive strength.

uncertainty about the other variables taken separately (Saltelli et al., 2008). Hence, concerning the nature of the output variables in this study, GSA is more rationale for examining the influence of input variables on the general model efficiency.

Among GSA techniques, a variance-based method was commonly used by researchers for SA. The technique provides an exact methodology for defining each ANN model input parameter's total and first-order sensitivity indices. Assuming a model with form $Y = f(X_1, X_2, \ldots, X_k)$

Table 6. statistical metrics of all developed informational model.

Informational model	All dataset			
	R^2	y = ax + b	AAE	VAF
SFLA-ANN	0.985	y = 1.0394x − 3.1655	0.030	0.982
GWO-ANN	0.953	y = 0.9619x + 2.0627	0.035	0.953
MLR	0.838	y = 0.8518x + 8.5788	0.074	0.838

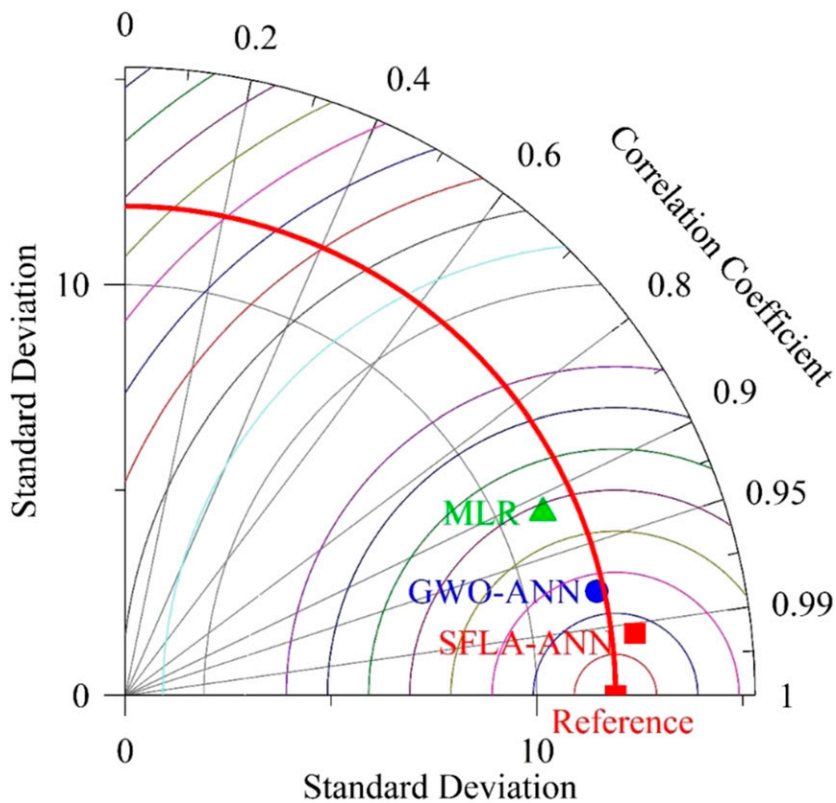

Figure 16. Taylor diagram visualization of SFLA-ANN model performance in the prediction of compressive strength.

in which Y is a scalar, to evaluate the impact of individual parameters, the variance-based method takes a variance ratio through variance decomposition based on equation (9):

$$V = \sum_{i=1}^{k} V_{\mathrm{i}} + \sum_{i=1}^{k} \sum_{j>i}^{k} V_{ij} + \ldots + V_{1,2,\ldots,k} \quad (8)$$

Where V is the variance of the output of the ANN model, V_i is the first-order variance of the input X_i, and V_{ij} to $V_{1,2,\ldots,k}$ signify the variance of the interface of the k parameters. V_i and V_{ij} denote the significance of the individual input to the output variance and are a function of the provisional expectation variance as determined from the following equations:

$$V_i = V_{x_i}[E_{x\sim i}(YX_i] \quad (9)$$

$$V_{ij} = V_{x_i x_j}\left[E_{x\sim ij}(YX_i, X_j\right] - V_i - V_j \quad (10)$$

with ?$_{\sim i}$ determines the set of all input variables in addition to X_i. The first-order sensitivity index (S_i) denotes the first-order effect of an input X_i on the global output using the following equation:

$$S_i = \frac{V_i}{V(Y)} \quad (11)$$

Results of the SA are depicted in Figure 17, which confirms that the FA/GBFS ratio significantly influences the compressive strength by a factor of 53%. The figure also shows that the second largest contributor to the compressive strength is the age of geopolymer concrete by 0.22%. Furthermore, the results indicate that the

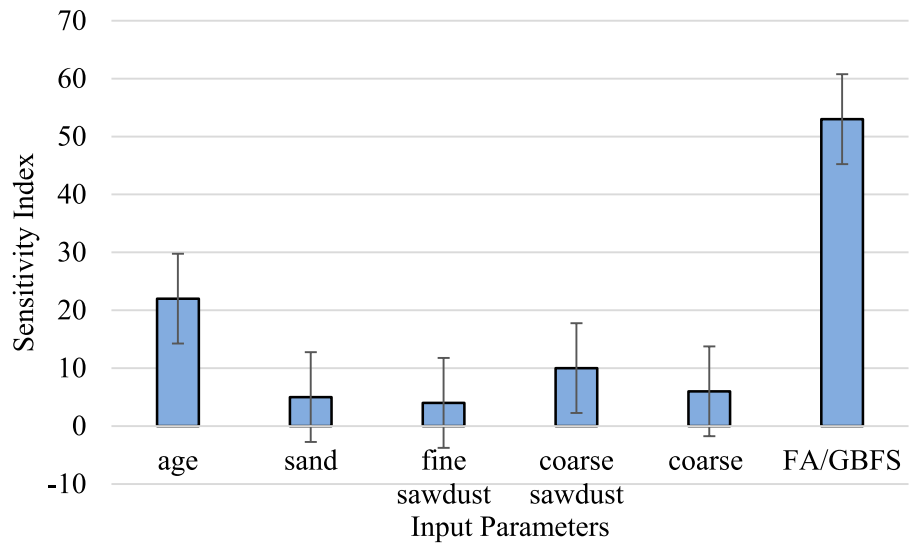

Figure 17. Sensitivity of compressive strength in sawdust-modified geopolymer concrete to the mix design parameters.

compressive strength of sawdust-modified geopolymer concrete was less sensitive to the content of natural aggregate substitution with sawdust aggregate, which had a significance of only 0.15%.

Conclusion

This study investigates the feasibility of utilizing sawdust as a natural fine and coarse aggregate substitution in FA-GBFS based geopolymer concrete. Several mixes with a different percentage of sawdust substituting natural aggregate were designed to examine the effects of sawdust on the mechanical properties of FA-GBFS-based geopolymer concrete. Besides, an informational model was developed using an experimental dataset to estimate the compressive strength of mix designs and their sensitivity to sawdust content. The following summarizes the main finding of this study.

1. The average slump value for conventional FA-GBFS based geopolymer concrete with natural aggregate was recorded at 140 mm, whereas by substituting all natural aggregate with sawdust, the slump decreased by around 55% and reached 75 mm.
2. The initial and final setting times of conventional geopolymer concrete with FA/GBFS ratio of 2.33 were recorded at 38 and 60 min, whereas by substituting all natural aggregate with sawdust, these values decreased by around 40% and were recorded at 25 and 43 min, respectively.
3. There is an indirect relationship between compressive strength and sawdust content where in conventional geopolymer concrete with FA/GBFS ratio of 2.33, the compressive strength was recorded at 50 MPa, and by substituting all natural aggregate with sawdust, this value declined by 35%, and was recorded 37 MPa.
4. The results confirm that sawdust-modified geopolymer concrete possessed a higher potential to absorb sound energy in the range varies 500–3000 Hz and lower thermal conductivity. By substituting all natural aggregate with sawdust, a time interval of 188 min was required for heat transfer compared to 36 min for specimen made with 100% natural aggregate.
5. The results confirm the higher reliability of the proposed SFLA-ANN model for estimating the compressive strength of modified-sawdust geopolymer concrete compared to the other informational models. The sensitivity analysis also proves that FA/GBFS ratio has a major impact of 53% on compressive strength, whereas it is less sensitive to the sawdust content by only 0.15%. This novel informational model attained superior accuracy and could be used to simplify the generative design in future computational intelligence construction building material platforms.

Declaration of conflicting interests

The author(s) declared no potential conflicts of interest with respect to the research, authorship, and/or publication of this article.

Funding

The author(s) received no financial support for the research, authorship, and/or publication of this article.

ORCID iDs

Iman Faridmer https://orcid.org/0000-0003-3307-3444
Chiara Bedon https://orcid.org/0000-0003-3875-2817

References

Adeli H (2001) Neural networks in civil engineering: 1989–2000. *Computer-Aided Civil and Infrastructure Engineering* 16: 126–142.

Adesina A (2020) Performance of fibre reinforced alkali-activated composites–A review. *Materialia* 12: 100782.

Aggregates BN-W ASTM C 33/C 33M, Class 4S, uniformly graded. *Provide aggregates from a single source* 1: 1.

Ahmed W, Khushnood RA, Memon SA, et al. (2018) Effective use of sawdust for the production of eco-friendly and thermal-energy efficient normal weight and lightweight concretes with tailored fracture properties. *Journal of Cleaner Production* 184: 1016–1027.

Al-Homoud DMS (2005) Performance characteristics and practical applications of common building thermal insulation materials. *Building and environment* 40: 353–366.

Alabduljabbar H, Huseien GF, Sam ARM, et al. (2020) Engineering properties of waste sawdust-based lightweight alkali-activated concrete: experimental assessment and numerical prediction. *Materials* 13: 5490.

Algaifi HA, Mustafa mohamed A, Alsuhaibani E, et al. 2021. Optimisation of GBFS, fly ash, and nano-silica contents in alkali-activated mortars. *Polymers*, 13, 2750.

Alharbi YR and Abadel AA (2022) Engineering properties of high-volume fly ash modified cement incorporated with bottle glass waste nanoparticles. *Sustainability* 14: 12459.

Aliabdo AA, Abd Elmoaty AEM and Abdelbaset MM (2015) Utilization of waste rubber in non-structural applications. *Construction and Building Materials* 91: 195–207.

Asaad MA, Huseien GF, Memon RP, et al. (2022) Enduring performance of alkali-activated mortars with metakaolin as granulated blast furnace slag replacement. *Case Studies in Construction Materials* 16: e00845.

ASTM (2015) *Standard Specification for Coal Fly Ash and Raw or Calcined Natural Pozzolan for Use in Concrete*. ASTM C618–15.

ASTM A (2020) C109/109M. *Standard Test Method for Compressive Strength of Hydraulic Cement Mortars*. *Using 2-In. or [50-mm] Cube Specimens)*.

ASTM C (2006) *Standard Test Method for Sieve Analysis of Fine and Coarse Aggregates*. *ASTM C136-06*.

Bagheri A and Nazari A (2014) Compressive strength of high strength class C fly ash-based geopolymers with reactive granulated blast furnace slag aggregates designed by Taguchi method. *Materials & Design* 54: 483–490.

Batool F, Islam K, Cakiroglu C, et al. (2021) Effectiveness of wood waste sawdust to produce medium-to low-strength concrete materials. *Journal of Building Engineering* 44: 103237.

Bishop CM (2006) *Pattern Recognition and Machine Learning*. Berlin: springer.

Brough A and Atkinson A (2002) Sodium silicate-based, alkali-activated slag mortars: Part I. Strength, hydration and microstructure. *Cement and Concrete Research* 32: 865–879.

Chowdary TB and Rao VR (2022) Design and analysis of lightweight alkali-activated slag and fly ash geopolymer mortars using ANFIS-SSO. *Iranian Journal of Science and Technology, Transactions of Civil Engineering* 46: 1211–1224.

Chowdhury S, Mishra M and Suganya O (2015) The incorporation of wood waste ash as a partial cement replacement material for making structural grade concrete: an overview. *Ain Shams Engineering Journal* 6: 429–437.

Clarke DR (2003) Materials selection guidelines for low thermal conductivity thermal barrier coatings. *Surface and Coatings Technology* 163-164: 67–74.

Deir E, Gebregziabiher BS and Peethamparan S (2014) Influence of starting material on the early age hydration kinetics, microstructure and composition of binding gel in alkali activated binder systems. *Cement and Concrete Composites* 48: 108–117.

Dixit A and Pang SD (2022) Optimizing lightweight expanded clay aggregate coating for enhanced strength and chloride resistance. *Construction and Building Materials* 321: 126380.

Duan P, Yan C and Luo W (2016) A novel waterproof, fast setting and high early strength repair material derived from metakaolin geopolymer. *Construction and Building Materials* 124: 69–73.

Duan P, Yan C, Zhou W, et al. (2015) An investigation of the microstructure and durability of a fluidized bed fly ash–metakaolin geopolymer after heat and acid exposure. *Materials & Design* 74: 125–137.

Efnarc S (2002) *Guidelines for Self-Compacting Concrete*. London, UK: Association House, Vol 32, p. 34.

Flood I and Kartam N (1994) Neural networks in civil engineering. I: principles and understanding. *Journal of computing in civil engineering* 8: 131–148.

Galdean N, Callisto M and Barbosa F (2000) Lotic ecosystems of Serra do Cipó, southeast Brazil: water quality and a tentative classification based on the benthic macroinvertebrate community. *Aquatic Ecosystem Health and Management* 3: 545–552.

Gao X, Yu Q and Brouwers H (2015a) Characterization of alkali activated slag–fly ash blends containing nano-silica. *Construction and Building Materials* 98: 397–406.

Gao X, Yu Q and Brouwers H (2015b) Properties of alkali activated slag–fly ash blends with limestone addition. *Cement and Concrete Composites* 59: 119–128.

Gao X, Yu Q and Brouwers H (2015c) Reaction kinetics, gel character and strength of ambient temperature cured alkali activated slag–fly ash blends. *Construction and Building Materials* 80: 105–115.

Granizo ML, Alonso S, Blanco-Varela MT, et al. (2004) Alkaline activation of metakaolin: effect of calcium hydroxide in the products of reaction. *Journal of the American Ceramic Society* 85: 225–231.

Haykin S (2007) *Neural Networks: A Comprehensive Foundation*. Hoboken, NJ: Prentice-Hall, Inc.

Huseien GF, Memon RP, Kubba Z, et al. (2019) *Mechanical, Thermal and Durable Performance of Wastes Sawdust as Coarse Aggregate Replacement in Conventional Concrete*. Jurnal Teknologi, Vol 81.

Institute AC (2011) *Building Code Requirements for Structural Concrete (ACI 318-11) and Commentary*. Farmington Hills, MI: ACI, 318R-11.

Islam A, Alengaram UJ, Jumaat MZ, et al. (2014) The development of compressive strength of ground granulated blast furnace slag-palm oil fuel ash-fly ash based geopolymer mortar. *Materials & Design* 56: 833–841.

Kantarcı F and Maraş MM (2022) Formulation of a novel nano TiO2-modified geopolymer grout for application in damaged beam-column joints. *Construction and Building Materials* 317: 125929.

Karamanova E, Avdeev G and Karamanov A (2011) Ceramics from blast furnace slag, kaolin and quartz. *Journal of the european ceramic society* 31: 989–998.

Khan EU, Khushnood RA and Baloch WL (2020) Spalling sensitivity and mechanical response of an ecofriendly sawdust high strength concrete at elevated temperatures. *Construction and Building Materials* 258: 119656.

Kockal NU and Ozturan T (2010) Effects of lightweight fly ash aggregate properties on the behavior of lightweight concretes. *Journal of hazardous materials* 179: 954–965.

Li F, Liu L, Yang Z, et al. (2021) Physical and mechanical properties and micro characteristics of fly ash-based geopolymer paste incorporated with waste Granulated Blast Furnace Slag (GBFS) and functionalized Multi-Walled Carbon Nanotubes (MWCNTs). *Journal of Hazardous Materials* 401: 123339.

Liang B, Zhen Z and Jiang J (2016) Modified shuffled frog leaping algorithm optimized control for air-breathing hypersonic flight vehicle. *International Journal of Advanced Robotic Systems* 13: 172988141667813.

Makhloufi Z, Chettih M, Bederina M, et al. (2015) Effect of quaternary cementitious systems containing limestone, blast furnace slag and natural pozzolan on mechanical behavior of limestone mortars. *Construction and Building Materials* 95: 647–657.

Maras MM (2021) Tensile and flexural strength cracking behavior of geopolymer composite reinforced with hybrid fibers. *Arabian Journal of Geosciences* 14: 2258.

Maras MM and Kose MM 2021. Structural behavior of masonry panels strengthened using geopolymer composites in compression tests. *Iranian Journal of Science and Technology, Transactions of Civil Engineering*, 45, 767-777.

Martínez-García C, González-Fonteboa B, Carro-López D, et al. (2019) Design and properties of cement coating with mussel shell fine aggregate. *Construction and Building Materials* 215: 494–507.

Memon RP, Sam ARM, Awal AA, et al. (2017) *Mechanical and Thermal Properties of Sawdust Concrete*. Jurnal Teknologi, Vol 79.

Mishra H and Jena A (2021) Light weight concrete using light weight expanded clay aggregate and dry saw dust. *Recent Developments in Sustainable Infrastructure*. Berlin: Springer.

Natephra W, Yabuki N and Fukuda T (2018) Optimizing the evaluation of building envelope design for thermal performance using a BIM-based overall thermal transfer value calculation. *Building and Environment* 136: 128–145.

Nikoo M, Hadzima-Nyarko M, Karlo Nyarko E, et al. (2018) Determining the natural frequency of cantilever beams using ANN and heuristic search. *Applied Artificial Intelligence* 32: 309–334.

Oyedepo OJ, Oluwajana SD and Akande SP (2014) Investigation of properties of concrete using sawdust as partial replacement for sand. *Civil and Environmental Research* 6: 35–42.

Palacios M and Puertas F (2007) Effect of shrinkage-reducing admixtures on the properties of alkali-activated slag mortars and pastes. *Cement and concrete research* 37: 691–702.

Palomo A, Grutzeck M and Blanco M (1999) Alkali-activated fly ashes: a cement for the future. *Cement and concrete research* 29: 1323–1329.

Papa E, Medri V, Landi E, et al. (2014) Production and characterization of geopolymers based on mixed compositions of metakaolin and coal ashes. *Materials & Design* 56: 409–415.

Park SB, Seo DS and Lee J (2005) Studies on the sound absorption characteristics of porous concrete based on the content of recycled aggregate and target void ratio. *Cement and Concrete Research* 35: 1846–1854.

Puertas F, Fernández-Jiménez A and Blanco-Varela MT (2004) Pore solution in alkali-activated slag cement pastes. Relation to the composition and structure of calcium silicate hydrate. *Cement and Concrete Research* 34: 139–148.

Rashad AM (2014) A comprehensive overview about the influence of different admixtures and additives on the properties of alkali-activated fly ash. *Materials & Design* 53: 1005–1025.

Rojo-López G, González-Fonteboa B, Martínez-Abella F, et al. 2022. Rheology, durability, and mechanical performance of sustainable self-compacting concrete with metakaolin and limestone filler. *Case Studies in Construction Materials* 17: e01143.

Ruiz-Santaquiteria C, Skibsted J, Fernández-Jiménez A, et al. (2012) Alkaline solution/binder ratio as a determining factor in the alkaline activation of aluminosilicates. *Cement and Concrete Research* 42: 1242–1251.

Sajedi F and Shafigh P (2012) High-strength lightweight concrete using leca, silica fume, and limestone. *Arabian journal for Science and engineering* 37: 1885–1893.

Saltelli A, Ratto M, Andres T, et al. (2008) *Global Sensitivity Analysis: The Primer*. Hoboken, NJ: John Wiley & Sons.

Sikora P, Rucinska T, Stephan D, et al. (2020) Evaluating the effects of nanosilica on the material properties of lightweight and ultra-lightweight concrete using image-based approaches. *Construction and Building Materials* 264: 120241.

Sosoi G, Abid C, Barbuta M, et al. (2022) Experimental investigation on mechanical and thermal properties of concrete using waste materials as an aggregate substitution. *Materials* 15: 1728.

Standard A C191-04b, (2004) "*Standard Test Methods for Time of Setting of Hydraulic Cement by Vicat Needle*," ASTM International, West Conshohocken, PA, 2004.

Standard A (2012) *ASTM C579: Standard Test Methods for Compressive Strength of Chemical-Resistant Mortars, Grouts, Monolithic Surfacings, and Polymer Concretes*. United States.

Standard A (2013) *C143: Standard Test Method for Slump of Hydraulic-Cement Concrete*. West Conshohocken, PA: Annual Book of ASTM Standards, ASTM International.

Trømborg E, Ranta T, Schweinle J, et al. (2013) Economic sustainability for wood pellets production–A comparative study between Finland, Germany, Norway, Sweden and the US. *Biomass and bioenergy* 57: 68–77.

Xu H and Van Deventer J (2000) The geopolymerisation of alumino-silicate minerals. *International journal of mineral processing* 59: 247–266.

Yahya Mohammed Al-Fasih M, Fahim Huseien G, Syahrizal bin Ibrahim I, et al. (2021) Synthesis of rubberized alkali-activated concrete: experimental and numerical evaluation. *Construction and Building Materials* 303: 124526.

Yusuf MO, Megat Johari MA, Ahmad ZA, et al. (2014a) Effects of H 2 O/Na 2 O molar ratio on the strength of alkaline activated ground blast furnace slag-ultrafine palm oil fuel ash based concrete. *Materials & Design* 56: 158–164.

Yusuf MO, Megat Johari MA, Ahmad ZA, et al. (2014b) Evolution of alkaline activated ground blast furnace slag–ultrafine palm oil fuel ash based concrete. *Materials & Design* 55: 387–393.

Yusuf MO, Megat Johari MA, Ahmad ZA, et al. (2014c) Influence of curing methods and concentration of NaOH on strength of the synthesized alkaline activated ground slag-ultrafine palm oil fuel ash mortar/concrete. *Construction and Building Materials* 66: 541–548.